ABUNDANT PO RADIOHALOS IN PHANEROZOIC GRANITES AND TIMESCALE IMPLICATIONS FOR THEIR FORMATION

Andrew A. Snelling — *Geo-Research Pty Ltd, P.O. Box 1208, Springwood, Queensland, 4127, Australia*

John R. Baumgardner — *Los Alamos National Laboratory, 1965 Camino Redondo, Los Alamos, NM 87544, USA*

Larry Vardiman — *Institute for Creation Research, PO Box 2667, El Cajon, CA 92021 USA*

Radiohalos are significant as a physical, integral, historical record of the decay of radioisotopes in their tiny central mineral inclusions. In thin section the typical dark concentric rings in the host minerals are due to the α-emissions, with the ring radii related to the distinctive α energies of the different radioisotopes in the ^{238}U and ^{232}Th decay series (Figure 1). ^{238}U and ^{232}Th radiohalos typically form around zircon and monazite inclusions, respectively, commonly in biotite, within granitic rocks (Figure 2). Radiohalos are also observed without central mineral inclusions and consisting only of rings from the last three α-emitters in the ^{238}U series: ^{218}Po, ^{214}Po and ^{210}Po (Figures 3 and 4). Because rings for all the Po precursors are missing, one infers there may have been migration of a Po precursor, most likely ^{222}Rn, away from a ^{238}U source in the genesis of such halos. Early research to understand how Po radiohalos might have formed focused on Precambrian granitic rocks. Thus it was claimed that the Po radiohalos were largely confined to such rocks. Furthermore, their formation was described as a "tiny mystery", because the half-lives for ^{218}Po of 3.1 minutes, ^{214}Po of 164 µs, and ^{210}Po of 138 days place severe time constraints on the processes for separating the Po precursor from parent ^{238}U and concentrating it and/or Po prior to halo formation.

We report new research which establishes that Po radiohalos are also common in Phanerozoic granites, for example, in the Lachlan Fold Belt of southeastern Australia and the Peninsular Ranges Batholith of southern California (Table 1). Their abundance is approximately ten ^{210}Po radiohalos for every ^{214}Po radiohalo, while ^{218}Po radiohalos are rare. The frequency of ^{238}U halos in these rocks is typically comparable to that of the ^{210}Po halos. Po halos are usually found in the same biotite grains as ^{238}U halos. The zircon inclusions in the latter often contain >100 ppm U and therefore represent a potentially adequate source of precursor ^{222}Rn and Po for the Po halos.

Hydrothermal fluids appear to play a critical role in the formation of these Po halos, both in nuclide transport and in chemical reactions to precipitate Po at localized sites (Figure 5). Because of α-track annealing, the halos can form only below 150°C. The time window for the required hydrothermal activity in the cooling granite hence would have been extremely short compared with the timescale of ^{238}U decay. As a consequence the amount of ^{222}Rn available during this brief cooling window falls far short of the amount required to generate the observed mature halos. We view this seeming paradox as a hint that nuclear decay processes may have been occurring more rapidly during the interval in which these granites were cooling.

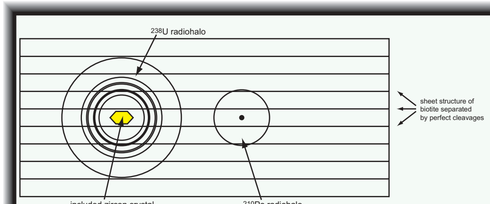

(a) Diagrammatic cross-section through a biotite flake showing the sheet structure and perfect cleavage. A tiny zircon crystal has been included between two sheets and its ^{238}U content has generated a ^{238}U radiohalo. A ^{210}Po radiohalo has also developed around a tiny radiocenter between the same two sheets.

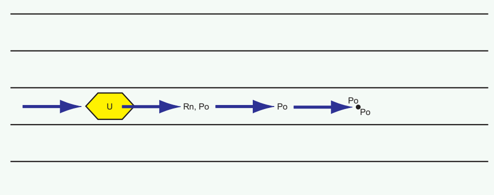

(d) As the temperatures approach 150°C and ^{222}Rn decays to ^{218}Po, the Po isotopes in the hydrothermal fluids, which have a geochemical affinity for S, precipitate to form PoS as the fluids flow past the S in the lattice defects. The U in the zircon continues to decay and replenish the supply of Rn and Po in the fluids.

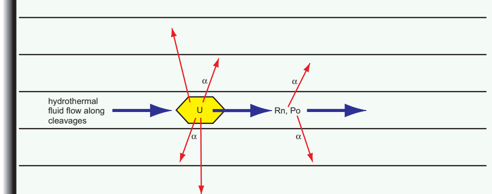

(b) Enlarged diagrammatic cross-section through a biotite flake that has crystallized from a granite magma to 300°C. The U in an included zircon crystal is emitting α-particles, while hydrothermal fluids released from the cooling magma are flowing along the cleavage plane dissolving decay products Rn and Po from the zircon and carrying them downflow where they also emit α-particles.

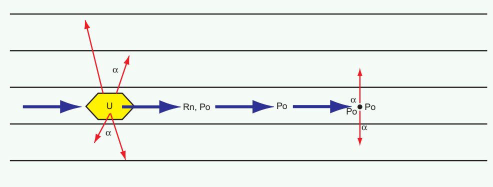

(e) Once the temperature drops to below 150°C, the α-tracks produced by continued decay of U in the zircon and of Po in the PoS are no longer annealed and so start discoloring the biotite sheets. More Po isotopes in the flowing hydrothermal fluids replace the Po in the PoS as it decays. There are not enough α-decays of Rn and Po in transit to also discolor the biotite sheets along the fluid flow path.

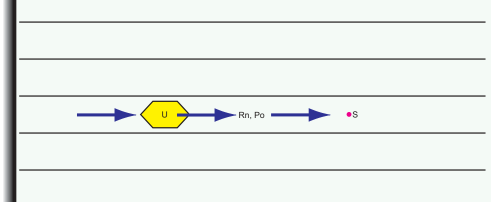

(c) However, at temperatures >150°C the α-tracks are annealed, so no radiohalos form and there is no α-track record of the hydrothermal fluids containing Rn and Po flowing along the cleavage plane. A few S atoms are in lattice defects downflow of the zircon crystal.

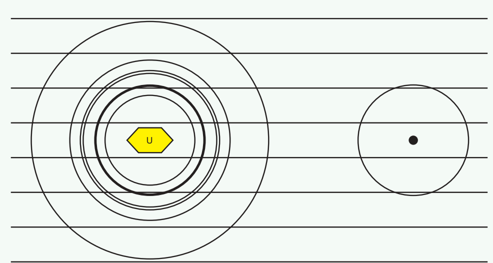

(f) With further passing of time and more α-decays both the ^{238}U and ^{210}Po radiohalos are fully formed, the granite cools completely and hydrothermal fluid flow ceases. Note that both radiohalos have to form concurrently below 150°C. The rate at which these processes occur must therefore be governed by the 138 day half-life of ^{210}Po. To get ^{218}Po and ^{214}Po radiohalos these processes would have to have occurred even faster.

Figure 5. **Time sequence of diagrams to show the formation of ^{238}U and ^{210}Po radiohalos concurrently.**

Rock Unit	Location	Age	Samples (slides)	Radiohalos ^{210}Po	^{214}Po	^{218}Po	^{238}U	^{232}Th
Indian Hill granites	San Diego	90 Ma	4 (180)	279	11	0	45	0
La Posta Pluton	County, CA	93 Ma	8 (383)	96	4	0	8	0
Granodiorite of Mono Dome	Yosemite, CA	93 Ma	1 (50)	6	0	0	0	0
San Jacinto Pluton	Palm Springs, CA	Late Cretaceous	9 (450)	96	0	0	9	0
Bass Lake Tonalite	Yosemite, CA	114 Ma	1 (50)	84	0	0	0	3
Ward Mountain Trondhjemite	Yosemite, CA	115 Ma	1 (50)	63	0	0	0	0
Granodiorite of Arch Rock	Yosemite, CA	114–117 Ma	2 (100)	106	0	0	7	10
Tonalite of the Gateway	Yosemite, CA	114–117 Ma	2 (100)	1	0	0	0	0
Wheeler Crest Granodiorite	Mammoth, CA	200–215 Ma	1 (50)	58	0	12	1	0
Lee Vining Canyon Granite	Yosemite, CA	200–215 Ma	1 (50)	108	0	2	13	0
Stanthorpe Adamellite	Queensland, Australia	232 Ma	1 (48)	520	4	15	68	19
Stone Mountain Pluton	Georgia	291±7 Ma	6 (291)	1109	93	2	88	0
Liberty Hill Pluton	Lancaster, SC	320 Ma	3 (150)	180	0	0	0	0
Bathurst Granite	New South Wales, Australia	330 Ma	1 (51)	45	0	0	3	0
Harcourt Granite	Victoria, Australia	369 Ma	1 (31)	107	130	0	198	0
Strathbogie Granite	Victoria, Australia	374 Ma	1 (50)	1366	232	1	1582	10
Shap Granite	Lake District, England	393 Ma	1 (55)	452	2	0	52	7
Shannons Flat Granite	New South Wales, Australia	417–443 Ma	1 (101)	9	18	0	38	0
Jillamatong Granite	New South Wales, Australia	417–443 Ma	1 (31)	120	118	0	137	0
Cootralantra Granite	New South Wales, Australia	417–443 Ma	1 (43)	230	75	0	276	2
Cooma Granodiorite	New South Wales, Australia	433 Ma	1 (41)	373	44	0	418	37
Encounter Bay Granite	South Australia	487–490 Ma	1 (45)	362	8	0	1586	161
Palmer Granite	South Australia	490 Ma	1 (51)	1352	17	0	631	3

Table 1. **Tabulation of radiohalo numbers counted in slides of mounted biotite flakes from granite samples spanning the Phanerozoic from Cambrian to Cretaceous, from southeastern Australia, California and southeastern USA, and northern England. Each slide contained more than 30 small biotite flakes, so at least 1000 small biotite flakes per sample were surveyed.**

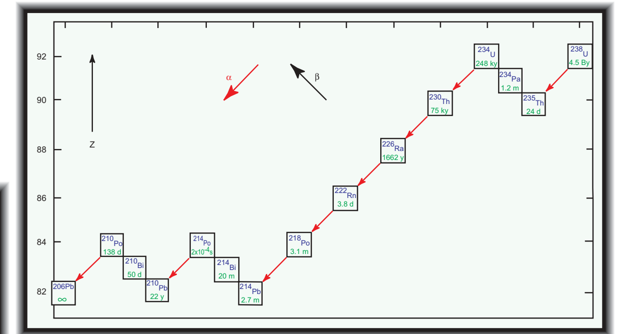

Figure 1. **Part of the chart of the nuclides showing the species in the ^{238}U decay series and their half-lives. Note the eight α-decayers, the Po isotopes being the last three.**

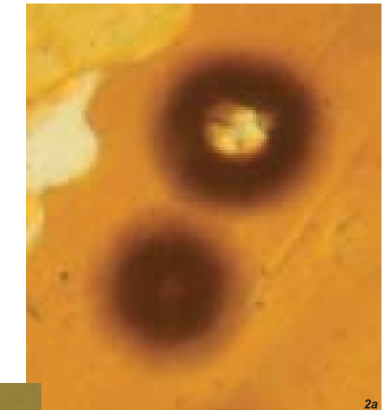

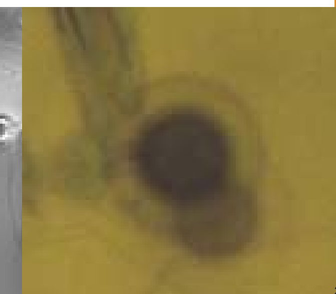

Figure 2. **^{238}U radiohalos in biotite flakes from granitic rocks. The diameters of the halos are approximately 60–70 µm.**
(a) Two ^{238}U radiohalos in the Silurian Cooma Granodiorite, Lachlan Fold Belt, southeastern Australia. The halos are overexposed so that the inner rings are indistinguishable. Within the upper halo the zircon radiocenter is visible, making the diameter of that halo slightly larger.
(b) Two ^{238}U radiohalos in the Ngaeri Granite, Japan. The inner rings are more easily distinguished, though the lower halo is faint.

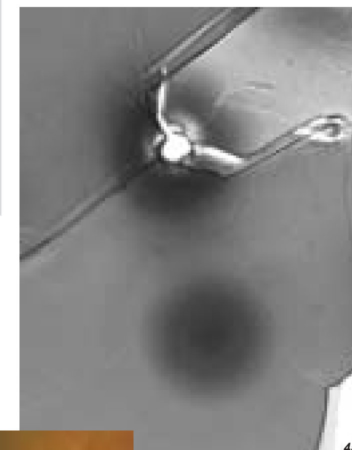

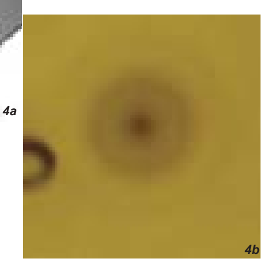

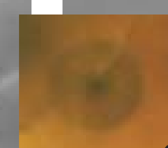

Figure 4. **Po radiohalos in biotite flakes from granitic rocks.**
(a) Two ^{214}Po radiohalos in the Triassic Stanthorpe Adamellite, New England Fold Belt, Queensland, Australia. The diameter of their outer rings is approximately 68 µm. The upper halo clearly has no visible inclusion for its radiocenter.
(b) A ^{218}Po radiohalo in the Ngaeri Granite, Japan. Its outer ring diameter is approximately 68 µm.
(c) A ^{210}Po radiohalo in the Carboniferous Stone Mountain Granite near Atlanta, GA. Its diameter is approximately 39 µm.
(d) A series of ^{218}Po radiohalos along a crack in a biotite flake from the Triassic Stanthorpe Adamellite, New England Fold Belt, Queensland, Australia. This confirms that the Po halos are of secondary origin due to hydrothermal fluid transport of the Po isotopes.

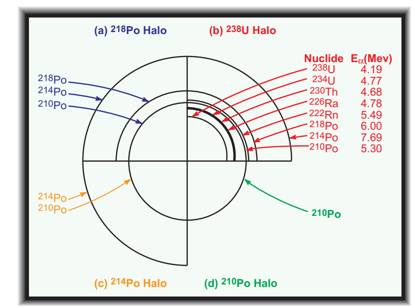

Figure 3. **Composite schematic drawing of (a) a ^{218}Po halo, (b) a ^{238}U halo, (c) a ^{214}Po halo, and (d) a ^{210}Po halo with radii proportional to the ranges of the α-particles in air. The nuclides responsible for the α-particles and their energies are listed for the different halo rings.**